Analysis of signed chromatic dispersion monitoring by waveform asymmetry for differentially-coherent phase-modulated systems

Alan Pak Tao Lau,[1] ZhaoHui Li,[2] F. N. Khan,[3] Chao Lu,[3] and P. K. A. Wai[3]

[1]*Photonics Research Center, Department of Electrical Engineering, The Hong Kong Polytechnic University, Hung Hom, Kowloon, Hong Kong*
[2]*Institute of Photonics Technology, Jinan University, China*
[3]*Photonics Research Center, Department of Electronic and Information Engineering, The Hong Kong Polytechnic University, Hung Hom, Kowloon, Hong Kong*
**eeaptlau@polyu.edu.hk*

Abstract: We analytically study received waveform asymmetries induced by chromatic dispersion (CD) for signed CD monitoring in differential quadrature phase-shift keying (DQPSK) systems and show that the asymmetries are results of differential detection and the $\pm\pi/4$ phase shifters used in conventional DQPSK receivers. The theoretical insights developed help explain various published results on signed CD monitoring based on waveform asymmetries and allow us to further propose signed CD monitoring for differential eight phase-shift keying (D8PSK) systems without any modification to the receiver. Simulation results also show that the CD-induced waveform asymmetric features are preserved in presence of self-phase modulation (SPM) and polarization-mode dispersion (PMD).

OCIS codes: (060.2330) Fiber optics communications; (060.5060) Phase modulation.

References and links

1. E. Ip, A. P. T. Lau, D. J. F. Barros, and J. M. Kahn, "Coherent Detection in optical fiber systems," Opt. Express **16**(2), 753–791 (2008).
2. W. Hatton and M. Nishimura, "Temperature dependence of chromatic dispersion in single mode fibers," J. Lightwave Technol. **4**(10), 15520–1555 (1986).
3. D. C. Kilper, R. Bach, D. J. Blumenthal, D. Einstein, T. Landolsi, L. Ostar, M. Preiss, and A. E. Willner, "Optical Performance Monitoring," J. Lightwave Technol. **22**(1), 294–304 (2004).
4. A. R. Chraplyvy, R. W. Tkach, L. L. Buhl and R. C. Alferness, "Phase modulation to amplitude modulation conversion of CW laser light in optical fibers," Electron. Lett. **22**(8), 409–411 (1986).
5. M. N. Petersen, Z. Pan, S. Lee, S. A. Havstad and A. E. Willner, "Online chromatic dispersion monitoring and compensation using a single inband subcarrier tone," IEEE Photon. Technol. Lett. **14**(4), 570–572 (2002).
6. T. E. Dimmick, G. Rossi and D. J. Blumenthal, "Optical Dispersion Monitoring Technique Using Double Sideband Subcarriers," IEEE Photon. Technol. Lett. **12**(7), 900–902 (2000).
7. G. Rossi, T. E. Dimmick, and D. J. Blumenthal, "Optical performance monitoring in reconfigurable WDM optical networks using subcarrier multiplexing," J. Lightwave Technol. **18**(12), 1639–1648 (2000).
8. K. J. Park, C. J. Youn, J. H. Lee, and Y. C. Chung, "Performance Comparisons of Chromatic Dispesion-Monitoring Techniques Using Pilot Tones," IEEE Photon. Technol. Lett. **15**(6), 873–875 (2003).
9. Z. Pan, Y. Xie, S. A. Havstad, Q. Yub, A. E. Willner, V. Grubsky, D. S. Starodubovc, and J. Feinberg, "Real-time group-velocity dispersion monitoring and automated compensation without modifications of the transmitter," Opt. Commun. **230**, 145–149 (2003).

#140759 - $15.00 USD Received 11 Jan 2011; revised 9 Feb 2011; accepted 9 Feb 2011; published 16 Feb 2011

10. N. Liu, W. Zhong, Y. Wen, and Z. Li, "New transmitter configuration for subcarrier multiplexed DPSK systems and its applications to chromatic dispersion monitoring," Opt. Express **15**(3), 839–844 (2007).
11. B. Fu and R. Hui, "Fiber chromatic dispersion and polarization-mode dispersion monitoring using coherent detection," IEEE Photon. Technol. Lett. **17**(7), 1561–1563 (2005).
12. Y. K. Lizé, J.-Y. Yang, L. Christen, X. Wu, S. Nuccio, T. Wu, A.E. Willner, R. Kashyap, and F. Seguin, "Simultaneous and Independent Monitoring of OSNR, Chromatic and Polarization Mode Dispersion for NRZ-OOK, DPSK and Duobinary," *OFC/NFOEC* 2007, Paper OThN2.
13. B. Kozicki, A. Maruta, and K. Kitayama, "Transparent performance monitoring of RZ-DQPSK systems employing delay-tap sampling," J. Opt. Netw. **6**, 1257–1269 (2007).
14. B. Kozicki, A. Maruta, and K. Kitayama, "Experimental Demonstration of optical performance monitoring for RZ-DPSK signal using delay tap sampling," Opt. Express **16**(6), 3566–3576 (2008).
15. T. Anderson, K. Clarke, D. Beaman, H. Ferra, M. Birk, G. Zhang, and P. Magill, "Experimental Demonstration of Multi-Impairment Monitoring on a commercial 10 Gbit/s NRZ WDM channel," *OFC/NFOEC* 2009, paper OTHh7.
16. Z. Li and G. Li, "In-line performance monitoring for RZ-DPSK signals using asynchronous amplitude histogram evaluation," IEEE Photon. Technol. Lett. **18**(3), 472–474 (2006).
17. D. Sandel, V. Mirvoda, F. Wust, R. Noe, and C.-J. Weiske, "Signed online chromatic dispersion detection at 40 Gbit/s based on arrival time detection with 60 attosecond dynamic accuracy," Electron. Lett. **38**(17), 984–985 (2002).
18. R. Noé, D. Sandel, S. Bhandare, F. Wst, B. Milivojevic, and V. Mirvoda, "Signed online chromatic-dispersion monitoring by synchronous detection of FM-induced arrival-time modulations in the clock-recovery phase-locked loop," J. Opt. Netw. **3**(8), 589–600 (2004).
19. Y. Takushima, H. Yoshimi, Y. Ozeki, K. Kikuchi, H. Yamauchi, and H. Taga, "In-Service Dispersion Monitoring in 32× 10.7 Gbps WDM Transmission System Over Transatlantic Distance Using Optical Frequency-Modulation Method," J. Lightwave Technol. **22**(1), 257–265 (2004).
20. N. Liu, W. Zhong, X. Yi, Y. Wang, and C. Lu, "Chromatic dispersion monitoring using the power ratio of two RF tones with a dispersion offset," *OFC* 2004, paper MF 81.
21. H. Kawakami, E. Yoshida, H. Kubota, and Y. Miyamoto, "Novel signed chromatic dispersion monitoring technique based on asymmetric waveform distortion in DQPSK receiver," *OECC* 2008, paper WeK-3.
22. Z. Li, J. Zhao, L. Cheng, Y. Yang, C. Lu, A. P. T. Lau, C. Yu, H. Y. Tam and P. K. A. Wai, "Signed CD Monitoring of 100-Gbit/s CS-RZ DQPSK Signal by Evaluating the Asymmetry Ratio of Delay-tap Sampling," Opt. Express **18**(3), 3149–3157 (2010).
23. J. Zhao, Z. Li, D. Liu, L. Cheng, C. Lu and H. Y. Tam, "NRZ-DPSK and RZ-DPSK Signals Signed Chromatic Dispersion Monitoring Using Asynchronous Delay-Tap Sampling," J. Lightwave Technol. **27**(23), 5295–5301 (2009).
24. Y. Han, C. Kim, and G. Li, "Simplified receiver implementation for optical differential 8-level phase-shift keying," Electron. Lett. **40**(21), 1372–1373 (2004).
25. K. J. Park, C. J. Youn, J. H. Lee, and Y. C. Chung, "Effect of self-phase modulation on group-velocity dispersion measurement technique using PM-AM conversion," Electron. Lett. **38**(21), 1247–1248 (2002).
26. C. Youn, "Effects of SPM and PMD on chromatic dispersion monitoring techniques using pilot tones," *OFC* 2003, paper WP2.

1. Introduction

Long-haul fiber-optic communication systems are currently moving towards differentially-coherent as well as coherent detection where the information is encoded in the phase of the optical carrier [1]. In particular, modulation formats such as polarization-multiplexed differential quadrature phase-shift keying (PM-DQPSK) are believed to be the standard for next-generation systems operating at 100 Gb/s and are currently under intensive research. Signal transmission in optical fibers is subjected to impairments such as chromatic dispersion (CD) and polarization-mode dispersion (PMD) which vary with temperature [2], component aging, fiber plant maintenance and dynamic routing in optical networks. Therefore, monitoring of the channel parameters such as CD is required for their appropriate compensation using optical or electronic techniques. Consequently, CD monitoring is a vital part of optical networks [3], especially for next-generation systems in which the tolerance to residual CD of the link decreases dramatically with increasing symbol rate.

Traditionally, CD can be monitored by phase-modulating the optical carrier [4] or inserting tones at the transmitter [5–8] and measuring the power of a CD-induced RF tone at the

#140759 - $15.00 USD Received 11 Jan 2011; revised 9 Feb 2011; accepted 9 Feb 2011; published 16 Feb 2011

receiver. Alternatively, such RF tone can be obtained from clock tones for pulse shapes such as Non Return-to-Zero (NRZ)-, Return-to-Zero (RZ)- and Carrier-Suppressed (CS)-RZ On-Off Keying (OOK) [9]. CD monitoring techniques for coherent or differentially-coherent systems have also been studied [10–16]. However, the majority of the proposed techniques are not able to distinguish between the sign of CD which is vital for residual CD compensation. Sandel [17], Noé [18] and Takushima [19] studied signed CD monitoring by amplitude modulating a CW laser and measuring the signal arrival time or frequency modulating a CW laser and measuring received power fluctuations. However, complicated phase-lock loops are required. Liu et al. [20] added an additional dispersion element at the receiver to induce asymmetric dependence of the power ratio between two received RF tones on the sign of CD. On the other hand, Kawakami [21] proposed the use of asymmetric waveform distortions as a simple signed CD monitoring technique for RZ-DQPSK systems and our previous works [22, 23] also exploited such asymmetric features for signed CD monitoring for DQPSK and DPSK systems. However, no in-depth study on the nature of this asymmetry has been undertaken and the applicability and limitations of signed CD monitoring using waveform asymmetry are mostly unknown.

In this paper, we analytically study received waveform asymmetries induced by CD for DQPSK signals and show that such asymmetries are results of differential detection and the presence of $\pm\pi/4$ phase shifters in conventional DQPSK demodulators. The theoretical insights developed thus explain the origins of waveform asymmetry obtained from DPSK receivers with an imperfectly tuned phase shifter [23]. In addition, the underlying principles can be similarly exploited for D8PSK systems without any modifications to the receiver. We study the use of delay-tap plots to exploit this asymmetry for signed CD monitoring through simulations and note that many other techniques can be used for exploiting the asymmetry. Furthermore, simulation results show that CD-induced waveform asymmetries are preserved in long-haul systems with SPM and PMD.

2. Waveform asymmetry for DQPSK systems in presence of chromatic dispersion

Consider a fiber-optic transmission system with transmitted signal

$$E_t(t) = \sum_{k=-\infty}^{\infty} x_k b(t-kT) \tag{1}$$

where $x_k \in \{1,-1,j,-j\}$ denotes QPSK symbols that are independent and identically distributed (i.i.d.) random variables, T is the symbol period and $b(t)$ is the pulse shape centered at $t=0$ which can be NRZ, RZ or CS-RZ. Polarization, multi-channel effects and self-phase modulation (SPM) are neglected for simplicity. In addition, noise from optical amplifiers and other components are also excluded in our analysis to highlight the origins of waveform asymmetry caused by CD. We note that the analytical derivations in this paper equally applies to general DMPSK systems.

A channel with CD can be modeled as a linear and time-invariant (LTI) system with transfer function

$$H(\omega) = e^{j\beta_2\omega^2 L/2} \tag{2}$$

where β_2 is the group velocity dispersion (GVD) parameter and L is the length of the fiber. In this case, the corresponding impulse response $h(t)$ is given by

$$h(t) = \sqrt{\frac{-1}{2\beta_2 L\pi}} e^{-j\left(\frac{t^2}{2\beta_2 L}+\frac{\pi}{4}\right)}. \tag{3}$$

#140759 - $15.00 USD Received 11 Jan 2011; revised 9 Feb 2011; accepted 9 Feb 2011; published 16 Feb 2011

Denoting the collective effect of optical band-pass filters along the transmission link and electrical low-pass filters at the receiver as a LTI system with impulse response $g(t)$, the received signal is given by

$$E_r(t) = \sum_{k=-\infty}^{\infty} x_k A(t-kT) \tag{4}$$

where

$$A(t) = b(t) * g(t) * h(t) = p(t) * h(t) = e^{-j\frac{\pi}{4}} \sqrt{\frac{-1}{2\beta_2 L\pi}} \int_{-\infty}^{\infty} p(\tau) e^{-j(t-\tau)^2/2\beta_2 L} d\tau \tag{5}$$

and $p(t) = b(t) * g(t)$ denotes the signal pulse shape with optical band-pass and electrical low-pass filtering. For DQPSK systems, $E_r(t)$ will be mixed with a delayed version of itself plus a $\pm\pi/4$ phase shift using a demodulator shown in Fig. 1. The delayed signal is given by

$$E_r(t-T) = \sum_{k=-\infty}^{\infty} x_k A(t-(k+1)T). \tag{6}$$

In this configuration, the output of the balanced receiver is given by

$$y_I(t) = \Re\mathfrak{e}\{e^{j\pi/4} E_r(t) E_r^*(t-T)\} \quad \text{and} \quad y_Q(t) = \Re\mathfrak{e}\{e^{-j\pi/4} E_r(t) E_r^*(t-T)\}. \tag{7}$$

We will focus on $y_I(t)$ for the rest of the paper and note that subsequent results will be similar

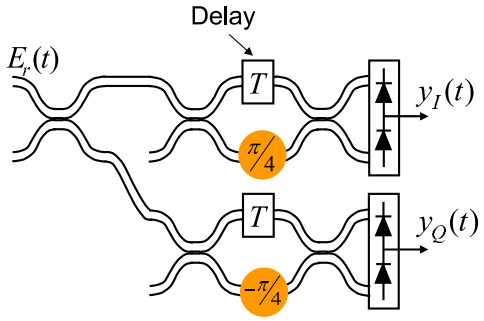

Fig. 1. Typical configuration for a DQPSK demodulator. $\pm\pi/4$ phase shifters in the two arms of the 3-dB couplers are used to detect the in-phase and quadrature component of the received signal. The T here represents one-bit delay.

to those from $y_Q(t)$. Now,

$$\begin{aligned} E_r(t)E_r^*(t-T) &= \Big(\sum_{k=-\infty}^{\infty} x_k A(t-kT)\Big)\Big(\sum_{k=-\infty}^{\infty} x_k A(t-(k+1)T)\Big)^* \\ &= \sum_{m=-\infty}^{\infty}\sum_{n=-\infty}^{\infty} x_m x_n^* A(t-mT)A^*(t-(n+1)T). \end{aligned} \tag{8}$$

The terms in Eq. (8) can be rewritten as

$$\begin{aligned} E_r(t)E_r^*(t-T) &= \sum_{k=-\infty}^{\infty} x_k x_{k-1}^* |A(t-kT)|^2 + \sum_{\substack{m,n=-\infty,\\ m\neq n,n+1}}^{\infty} x_m x_n^* A(t-mT)A^*(t-(n+1)T) \\ &\quad + \sum_{k=-\infty}^{\infty} A(t-kT)A^*(t-(k+1)T). \end{aligned} \tag{9}$$

#140759 - $15.00 USD Received 11 Jan 2011; revised 9 Feb 2011; accepted 9 Feb 2011; published 16 Feb 2011

In Eq. (9), the terms in the first line correspond to differentially encoded information to be detected and products of each individual pulse with the conjugate of its delayed self. As the expected value of two information symbols

$$\mathbf{E}[x_m x_n^*] = \begin{cases} 1 & n = m \\ 0 & n \neq m \end{cases},$$

the expected value of the balanced detector output is given by

$$\begin{aligned} \mathbf{E}[y_I(t)] &= \mathbf{E}[\mathfrak{Re}\{e^{j\pi/4} E_r(t) E_r^*(t-T)\}] \\ &= \sqrt{\frac{1}{2}}\mathfrak{Re}\Big\{ \sum_{k=-\infty}^{\infty} A(t-kT)A^*(t-(k+1)T) \Big\} \\ &\quad + \sqrt{\frac{1}{2}}\mathfrak{Im}\Big\{ \sum_{k=-\infty}^{\infty} A(t-kT)A^*(t-(k+1)T) \Big\} \end{aligned} \tag{10}$$

where $\mathfrak{Re}\{\cdot\}$ and $\mathfrak{Im}\{\cdot\}$ correspond to real and imaginary part respectively. If we let

$$z(t-kT) = A(t-kT)A^*(t-(k+1)T) + A(t-(k-1)T)A^*(t-kT),$$

then

$$\mathbf{E}[y_I(t)] = \frac{1}{2\sqrt{2}} \sum_{k=-\infty}^{\infty} \Big(\mathfrak{Re}\{z(t-kT)\} + \mathfrak{Im}\{z(t-kT)\} \Big). \tag{11}$$

Since $\mathbf{E}[y_I(t)]$ is periodic with period T, we will just focus on the symbol centered at $t = 0$ and consider the term $z(t) = A(t)A^*(t-T) + A(t+T)A^*(t)$. Now,

$$\begin{aligned} A(t)A^*(t-T) &= \frac{1}{2|\beta_2|L\pi} \iint p(\tau_1) p^*(\tau_2) e^{\frac{-j}{2\beta_2 L}[(t-\tau_1)^2 - (t-T-\tau_2)^2]} d\tau_1 d\tau_2 \\ &= \frac{1}{2|\beta_2|L\pi} \iint p(\tau_1) p(\tau_2) e^{\frac{-j}{2\beta_2 L}[(t-\tau_1)^2 - (t-T-\tau_2)^2]} d\tau_1 d\tau_2 \end{aligned} \tag{12}$$

as $p(t)$ is real for practical pulse shapes and filters. In this case, let

$$w_1(t) = \mathfrak{Im}\{A(t)A^*(t-T)\} = \frac{1}{2|\beta_2|L\pi} \iint p(\tau_1) p(\tau_2) \sin\Big(\frac{(t-T-\tau_2)^2 - (t-\tau_1)^2}{2\beta_2 L} \Big) d\tau_1 d\tau_2 \tag{13}$$

and

$$w_2(t) = \mathfrak{Im}\{A(t+T)A^*(t)\} = \frac{1}{2|\beta_2|L\pi} \iint p(\tau_1) p(\tau_2) \sin\Big(\frac{(t-\tau_1)^2 - (t+T-\tau_2)^2}{2\beta_2 L} \Big) d\tau_1 d\tau_2. \tag{14}$$

Now, we note that

$$w_1(-t) = \frac{1}{2|\beta_2|L\pi} \iint p(\tau_1) p(\tau_2) \sin\Big(\frac{(-t-T-\tau_2)^2 - (-t-\tau_1)^2}{2\beta_2 L} \Big) d\tau_1 d\tau_2. \tag{15}$$

If we re-define the dummy variables of integration $\tau_3 = -\tau_1$ and $\tau_4 = -\tau_2$,

$$\begin{aligned} w_1(-t) &= \frac{1}{2|\beta_2|L\pi} \iint p(-\tau_3) p(-\tau_4) \sin\Big(\frac{(-t-T+\tau_4)^2 - (-t+\tau_3)^2}{2\beta_2 L} \Big) d\tau_3 d\tau_4 \\ &\overset{(a)}{=} \frac{1}{2|\beta_2|L\pi} \iint p(\tau_3) p(\tau_4) \sin\Big(\frac{(t+T-\tau_4)^2 - (t-\tau_3)^2}{2\beta_2 L} \Big) d\tau_3 d\tau_4 \\ &= -w_2(t). \end{aligned} \tag{16}$$

#140759 - $15.00 USD Received 11 Jan 2011; revised 9 Feb 2011; accepted 9 Feb 2011; published 16 Feb 2011

where the equality in (a) stems from the fact that any practical pulse shape is symmetric about its center. Similarly, one can show that $w_2(-t) = -w_1(t)$ and therefore

$$\mathfrak{Im}\{z(t)\} = w_1(t) + w_2(t) = \mathfrak{Im}\{A(t)A^*(t-T)\} + \mathfrak{Im}\{A(t+T)A^*(t)\} \tag{17}$$

is an odd function of t and hence asymmetric about $t = 0$. On the other hand, it can be shown that $\mathfrak{Re}\{z(t)\}$ is an even function of t and will not result in any waveform asymmetry. Since the sum of an symmetric and asymmetric waveform is still asymmetric, we have just shown that the expected value of the received waveform $\mathbf{E}[y_I(t)]$ of a DQPSK demodulator exhibits an asymmetry about the center of each bit. Furthermore, $\mathfrak{Im}\{z(t)\}$ and $\mathfrak{Re}\{z(t)\}$ is also an odd and even function of β_2 respectively. Therefore, any waveform asymmetric feature for a given β_2 will be reversed about the center of the bit when the sign of β_2 is changed. Such asymmetry reversal is exactly the feature that allows one to distinguish the sign of CD from the received waveform. To illustrate the analytical insights with an example, consider the transmission of a pulse train with Gaussian pulse shape

$$b(t) = e^{-(t/T_o)^2}.$$

Neglecting the effect of optical and electrical filters for simplicity, it can be shown that

$$A(t) = \frac{T_o}{(T_o^2 - j\beta_2 L)^{1/2}} e^{-\frac{t^2}{2(T_o^2 - j\beta_2 L)}} = \frac{T_o}{(T_o^2 - j\beta_2 L)^{1/2}} e^{-ut^2 - j\beta_2 vt^2}$$

where $u = \frac{T_o^2}{2(T_o^4 + (\beta_2 L)^2)}$ and $v = \frac{L}{2(T_o^4 + (\beta_2 L)^2)}$. In this case,

$$\begin{aligned}
\mathrm{Im}\{z(t)\} &= \frac{1}{2\sqrt{2}} \frac{T_o^2}{\left(T_o^4 + (\beta_2 L)^2\right)^{1/2}} e^{-2ut^2 - uT^2} \times \\
&\quad \left[e^{-2utT}\mathrm{Im}\{e^{-j\beta_2 v[-(t+T)^2 + t^2]}\} + e^{2utT}\mathrm{Im}\{e^{-j\beta_2 v[-t^2 + (t-T)^2]}\}\right] \\
&= \frac{-1}{\sqrt{2}} \frac{T_o^2}{\left(T_o^4 + (\beta_2 L)^2\right)^{1/2}} e^{-2ut^2 - uT^2} \times \\
&\quad \left[\cosh(2utT)\sin(2vT\beta_2 t)\cos(\beta_2 vT^2) - \sinh(2utT)\cos(2vT\beta_2 t)\sin(\beta_2 vT^2)\right].
\end{aligned} \tag{18}$$

Note that $\mathrm{Im}\{z(t)\}$ is an odd function of t and β_2 and is shown in Fig. 2 for a 20G Sym/s system with $T_o = 15$ ps and $\pm$ 136 ps/nm of accumulated CD. It is clear from Eq. (18) that when the sign of β_2 changes, the direction of asymmetry also changes, enabling one to distinguish the sign of CD from the received waveform. As $y_I(t)$ is an ergodic process, the ensemble average $\mathbf{E}[y_I(t)]$ will be equal to the time-averaged waveform of one particular random realization of $y_I(t)$ and therefore the CD-induced asymmetric features can be extracted from an eye diagram.

Note that $\mathbf{E}[y_I(t)]$ is non-zero only because of the second line of Eq. (9) i.e. the product of each individual pulse with the conjugate of its delayed self. Consequently, CD-induced waveform asymmetries should only be present for differentially-coherent phase-modulated systems and not present for coherent modulation formats such as BPSK, QPSK or 16-Quadrature Amplitude Modulation(QAM). In addition, the asymmetry is due to the presence of the term $\sum_{k=-\infty}^{\infty} \mathfrak{Im}\{z(t-kT)\}$ which is brought about by the $\pm\pi/4$ phase shifters used in a typical DQPSK demodulator. The two above insights together explain the waveform asymmetries reported in [21,22] for DQPSK systems. Furthermore, they also explain how an intentional phase

#140759 - $15.00 USD Received 11 Jan 2011; revised 9 Feb 2011; accepted 9 Feb 2011; published 16 Feb 2011

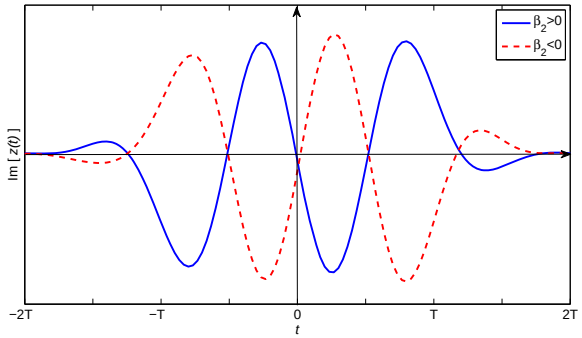

Fig. 2. The term $\mathrm{Im}\{z(t)\}$ for a 40Gb/s (20GSym/s) RZ-DQPSK system with Gaussian pulse shape and $\pm$136 ps/nm of accumulated CD. For a given CD value, the waveform is an odd function of t and hence asymmetric about $t = 0$. In addition, since $\mathrm{Im}\{z(t)\}$ is also an odd function of β_2, the direction of the time asymmetry will be reversed when the sign of β_2 is changed, thus explaining the observed waveform asymmetry that changes with the sign of accumulated CD.

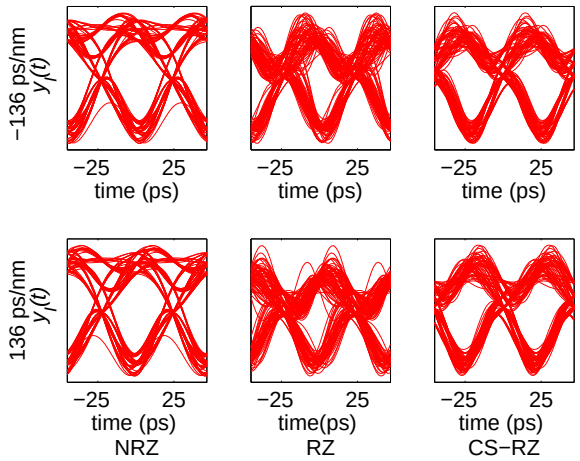

Fig. 3. Received eye diagrams for 40 Gb/s (20 GSym/s) DQPSK systems with various pulse shapes and residual dispersion of $\pm$136 ps/nm. The eyes are asymmetric about their centers and such asymmetries change with the sign of β_2.

mismatch of $\pi/4$ in one arm of a DPSK receiver enables signed CD monitoring for DPSK systems [23]. In addition, Fig. 3 shows the received eye diagrams for 40 Gb/s (20 GSym/s) NRZ-, RZ- and CS-RZ-DQPSK systems with an accumulated dispersion of $\pm$136 ps/nm obtained from simulations. Noises from lasers, optical amplifiers and receiver circuitries are neglected to illustrate the CD-induced waveform asymmetries. From the figure, it can be seen that asymmetries are present for all pulse shapes. This is in agreement with expectations as the analytical derivations above only assume the pulse shape $p(t)$ to be real and symmetric about its center. Therefore, the waveform asymmetric features should be present for all types of pulse shapes

#140759 - $15.00 USD Received 11 Jan 2011; revised 9 Feb 2011; accepted 9 Feb 2011; published 16 Feb 2011

commonly used in communication systems.

3. Signed CD monitoring for D8PSK systems using delay-tap sampling

The theoretical insights developed above indicate that CD-induced waveform asymmetry will be present as long as the modulation format is differentially-coherent and $\pm\pi/4$ phase shifters are used in the receiver structures. In fact, Eqs. (10) and (11) actually suggest that the term $\sum_{k=-\infty}^{\infty} \Im\mathfrak{m}\{z(t-kT)\}$, which causes the asymmetry, will be present as long as the phase shift of the 3-dB coupler is not 0. Consequently, for a D8PSK system with proposed receiver structures [24] such as the one shown in Fig. 4, one should be able to exploit the waveform asymmetric features in similar manners for signed CD monitoring.

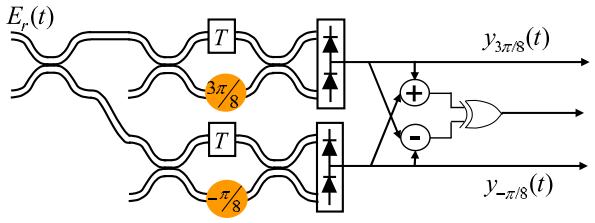

Fig. 4. D8PSK receiver configuration using two 3-dB couplers with $-\pi/8$ and $3\pi/8$ phase shifters followed by simple digital logic circuits. The output signals $y_{3\pi/8}(t)$ and $y_{-\pi/8}(t)$ can be used for signed CD monitoring.

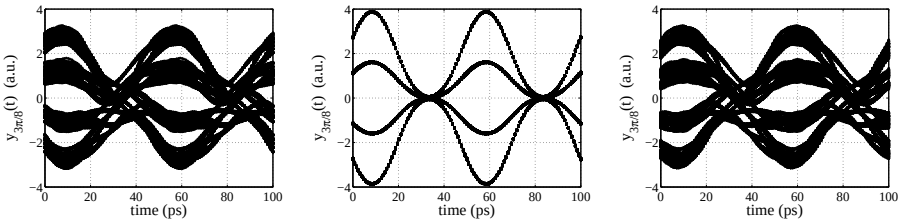

Fig. 5. Eye diagrams corresponding to the received signal $y_{3\pi/8}(t)$ for a 60 Gb/s (20 GSym/s) RZ-D8PSK system with (a) -136 ps/nm (b) 0 ps/nm and (c) 136 ps/nm of residual CD.

In particular, one of the balanced-detector output can be 'tapped' for signed CD monitoring without modifying the receiver structure. Fig. 5 shows the eye diagrams corresponding to the output signal $y_{3\pi/8}(t)$ of a 60 Gb/s (20 GSym/s) RZ-D8PSK system with -136 ps/nm, 0 ps/nm and 136 ps/nm of CD, indicating the presence of CD-induced waveform asymmetry. Similar to our previous studies, one can generate delay-tap plots from $y_{3\pi/8}(t)$ or $y_{-\pi/8}(t)$, evaluate the distances of sample pairs d_1, d_2 furthest away on both sides of the diagonal D and calculate the distance ratio d_1/d_2 for signed CD monitoring [22, 23]. Some delay-tap plots generated from $y_{3\pi/8}(t)$ are shown in Fig. 6 and the distance ratio d_1/d_2 vs. CD is shown in Fig. 7. It can be seen that the distance ratio corresponding to $y_{-\pi/8}(t)$ is not as sensitive to CD compared with that from $y_{3\pi/8}(t)$. This is in agreement with theoretical predictions as the coefficient of

#140759 - $15.00 USD Received 11 Jan 2011; revised 9 Feb 2011; accepted 9 Feb 2011; published 16 Feb 2011

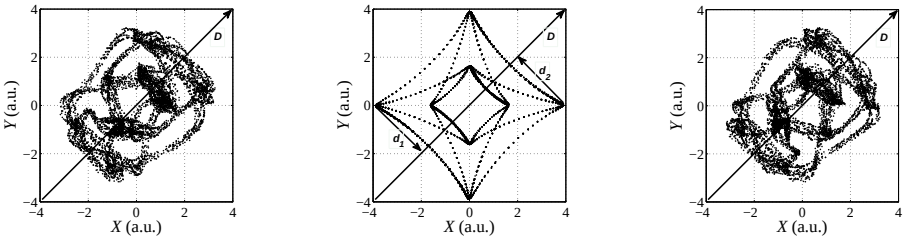

Fig. 6. Delay-tap plots obtained from the received signal $y_{3\pi/8}(t)$ for a 60 Gb/s (20 GSym/s) RZ-D8PSK system with (a) -136 ps/nm (b) 0 ps/nm and (c) 136 ps/nm of residual CD with delay value $\tau = 24$ ps. The distances d_1, d_2 of sample pairs furthest away from both sides of the diagonal D (shown in (b))can be used to calculate a distance ratio d_1/d_2 for signed CD monitoring.

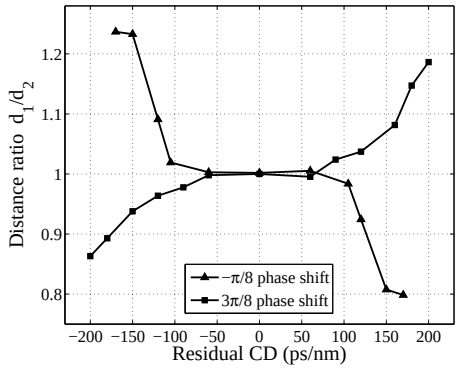

Fig. 7. Distance ratio d_1/d_2 as a function of residual CD for a 60 Gb/s (20 GSym/s) RZ-D8PSK system. The distance ratio obtained from $y_{3\pi/8}(t)$ is more sensitive to residual CD compared with that from $y_{-\pi/8}(t)$.

$\sum_{k=-\infty}^{\infty} \Im\mathfrak{m}\{z(t-kT)\}$ in Eqs. (10) and (11) will become large when the phase shift of the 3-dB coupler deviates away from 0. Moreover, in addition to delay-tap plots, we emphasize that many other techniques such as amplitude histograms and artificial neural networks can also be used to extract the CD-induced waveform asymmetric features for signed CD monitoring.

4. CD-induced waveform asymmetry in presence of SPM and PMD

In long-haul systems, signal transmission will also be affected by SPM as well as PMD and the performance of any CD monitoring technique maybe affected [25, 26]. To investigate the applicability of the signed CD monitoring technique for long-haul systems, Fig. 8 shows the distance ratio as a function of residual CD obtained from simulations for a 40 Gb/s RZ-DQPSK system with length 500 km and 1000 km. The transmission link consists of multiple spans of fiber with span length around 60 km and dispersion compensating fibers at each span such that the accumulated residual CD is equally distributed across the spans. The coarse-step model with 1-km step size is used for the simulation and the birefringence is random across different sections. The birefringence beat length is 15 m. The distance ratio corresponding to a link

#140759 - $15.00 USD Received 11 Jan 2011; revised 9 Feb 2011; accepted 9 Feb 2011; published 16 Feb 2011

without SPM and PMD is also shown as reference. The input power, fiber nonlinear coefficient γ and the PMD coefficient is 0 dBm, $1.2/W \cdot \text{km}$ and 0.1 ps/$\sqrt{\text{km}}$ respectively. From the figure, it can be seen that the CD-induced asymmetric features are still present for systems with SPM and PMD. Although the mapping between the distance ratio and residual CD will generally be different than the case without SPM and PMD and may need to be calibrated for each system setup, such mappings will still be able to distinguish between positive and negative CD. Consequently, the proposed signed CD monitoring technique will be applicable in realistic long-haul systems with high data rates in which residual CD compensation plays an important role in the overall performance of the transmission link.

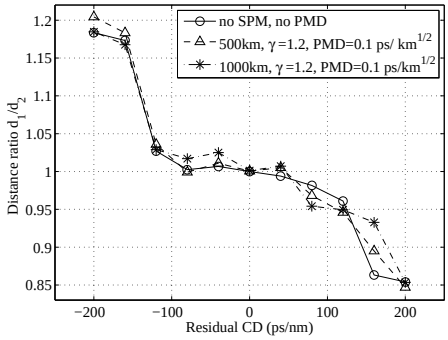

Fig. 8. Distance ratio d_1/d_2 as a function of residual CD for a 40 Gb/s RZ-DQPSK system in presence of SPM and PMD.

5. Conclusions

In this paper, we analytically studied signed CD monitoring using waveform asymmetries for DQPSK systems and showed that such asymmetries are results of differential detection and $\pm\pi/4$ phase shifters present in conventional DQPSK receivers. The theoretical insights developed help elucidate the operating principles behind other signed CD monitoring techniques based on waveform asymmetries reported in the literature and naturally suggest that similar methods can be used for D8PSK systems without modifications to the receiver. Signed CD monitoring using delay-tap plots is investigated for D8PSK systems through simulations and results are in agreement with theoretical predictions. In addition, the asymmetric features are shown to be preserved in presence of SPM and PMD and therefore the proposed technique can be used for signed CD monitoring in practical long-haul systems.

Acknowledgements

The authors would like to acknowledge the support of the Hong Kong Government General Research Fund (GRF) under project number PolyU 519910 and the Open Project of State Key Laboratory of Advanced Optical Communication Systems and Networks (2008SH04) of the People's Republic of China.